Journal of Materials Chemistry A

Accepted Manuscript

ROYAL SOCIETY OF CHEMISTRY

www.rsc.org/materialsA

Journal Name

ARTICLE

Solution-Processed Multilayered $BiVO_4$ Photoanodes: Influence of Intermediate Heat Treatments on the Photoactivity

Received 00th January 20xx,
Accepted 00th January 20xx

DOI: 10.1039/x0xx00000x

www.rsc.org/

A. Chemseddine*, K. Ullrich, T. Mete, F.F. Abdi, R. van de Krol

Spin coating of successive layers is a convenient method for fabricating metal oxide photoelectrodes with tunable thickness from a precursor solution. In this study, the crystallization behavior and photoelectrochemical properties of spin-coated $BiVO_4$ films are investigated as a function of the brief heat treatments applied after depositing each individual layer. We find that full crystallization of the final films can only be obtained when the films are subjected to 10 min. intermediate heat treatments to at least 350°C. Heat treatments at lower temperatures result in films which remain partially amorphous, even after final treatment at 460 °C. For intermediate heat treatments above 350 °C the layers fully crystallize to the desired monoclinic scheelite phase, showing improved carrier separation efficiencies but lower efficiencies for charge injection into the electrolyte. These findings suggest that choosing the right processing conditions is an essential first step towards improving the performance of solution-processed $BiVO_4$ photoelectrodes.

1. Introduction

The production of hydrogen through photocatalytic or photoelectrocatalytic water splitting is an attractive solution for storing solar energy and therefore to overcome the discontinuous availability of sunlight[1]. Since the discovery of this concept, half a century ago, by Fujishima and Honda using rutile TiO_2 decorated with platinum particles as a photoelectrode in a chemically-biased water splitting cell[2], scientists have been looking for ways to increase efficiency of this process using other materials[3-5]. In the last few years, many research groups have been working on $BiVO_4$-based photoanodes[6-13]. A variety of techniques have been used to synthesize these films, such as sputtering[7,8], spray pyrolysis[9,10], spin-coating[11,12] as well as wet-chemical methods using different precursors [6]. In many reports authors were able to significantly improve the efficiency through doping[13-15], nanostructuring[16,17], using Al-doped ZnO as electron collector[18], Plasmonic enhancement in photonic crystals[19] and by adding a co-catalyst[10-13]. However, these reports usually began with un-modified pure $BiVO_4$ that shows large variations in photocurrent. These variations can presumably be attributed to changes in the thickness, porosity, texture, stoichiometry, etc., but the influence of the synthesis procedure on these parameters is still poorly understood.

The aim of this contribution is to identify some of the critical parameters that affect the photoactivity of solution-processed $BiVO_4$ films. To control the thickness of these films, they are generally made by depositing multiple layers in succession, with intermediate heat treatments to dry and, if desired, pre-crystallize the individual layers. Although the intermediate heat treatment of these individual layers is likely to have a major influence on the overall performance of the films, little attention has yet been paid to this processing step.

Here, we systematically investigate the influence of the temperature used during heat treatment of the individual layers. To minimize the influence of other process parameters, the $BiVO_4$ layers were prepared in exactly the same way by spin-coating, using the same precursor solution and the same final high-temperature anneal. The results show that the intermediate heat treatment of the individual layers is a critically important step in the processing of efficient $BiVO_4$ photoanodes.

2. Experimental section

$BiVO_4$ multilayer photoanodes were fabricated by spin-coating successive layers. The precursor solution was prepared by dissolving bismuth (III) acetate (Alfa Aesar, 99%) in a 1:1 mixture (by volume) of acetic acid (J.T Baker, 99-100%), and methoxyethanol (99,3%, Sigma-Aldrich), and by adding an equimolar amount of vanadium(V) oxytrisopropoxide (Sigma-Aldrich, 99.9%) in methoxyethanol. A clear yellow transparent solution containing 20 mM/l of bismuth and 20 mM/l of vanadium, in a 4:1 (by volume) mixture methoxyethanol/acetic acid, was obtained. The bismuth concentration was kept constant in all precursor solutions. The solution (150 µl) was

[a] Institute for Solar Fuels, Helmholtz-Zentrum Berlin für Materialien und Energie GmbH, Hahn-Meitner-Platz 1, 14109 Berlin (Germany)

*E-Mail:Chemseddine@helmholtz-berlin.de

deposited onto FTO substrates by spin coating at 2000 rpm followed by pre-heating at various temperatures (T_{PR}) for 10 min in a preheated furnace. The spin-coating procedure was repeated multiple times to obtain the desired thickness, as illustrated schematically in Figure 1, with the same 10 min. heat treatment step after each layer. After applying the final layer, the electrodes were heated to a final temperature of 460 °C for two hours. Different films were made by changing T_{PR} to 150 °C, 200 °C, 250°C, 300°C, 350°C and 400°C, while keeping all other parameters the same. The heating under oxygen was performed at a rate of 40 mL/min. Humidified oxygen was prepared by passing it through water via a tube in a 0.5L gas washing bottle by keeping the same rate.

The $BiVO_4$ electrodes obtained after calcination at 460 °C were characterized by X-ray diffraction using a PANalytical X´pert PRO MRD with a Cu-Kα source in a grazing incidence configuration at different incident angles of 0.1°, 0.3° and 0.5° (see supporting information). Highly crystalline $BiVO_4$ films directly grown by a slightly modified chemical bath technique[28] on a $BiVO_4$ seed film were used for comparison, details are shown in the supporting information. The morphology of the electrodes was characterized by scanning electron microscopy using a Leo Gemini 1530 microscope.

Photoelectrochemical characterization was carried out in an aqueous 0.5 M K_2SO_4 (99%, Merck) solution buffered to pH ~5.6 with 0.09 M KH_2PO_4 (99% Merck) and 0.01 M K_2HPO_4 (99%, Merck) and 0.5 M H_2O_2. White light photocurrent measurements were performed under simulated AM1.5 solar illumination (100 mW/cm^2) with a Wacom Class AAA solar simulator (type WXS-50S-5H).

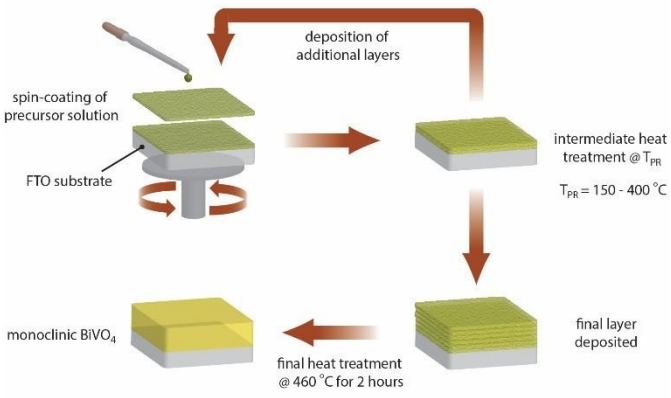

Figure 1. Schematic illustration of the process used to make the multilayer films.

The potential of the working electrode was controlled by a potentiostat (EG&G PAR 273) in a three-electrode configuration, with a Pt wire and an Ag/AgCl electrode (XR300, saturated KCl and AgCl solution; Radiometer Analytical) as the counter and reference electrodes, respectively.

3. Results and discussion

3.1 Characterization of $BiVO_4$ electrodes

X-ray diffraction patterns of $BiVO_4$ films consisting of 8 spin-coated layers were taken at different incident angles. Figure 2a shows spectra taken at a 0.1° incidence angle of films processed at different T_{PR}. An XRD spectrum for a $BiVO_4$ film grown by chemical bath deposition (CBD) is also shown. All samples show the presence of the monoclinic $BiVO_4$ crystal phase, without any evidence for other Bi- or V-containing phases. Additional peaks due to the underlying FTO substrate, indicated by asterisks, are also present. In addition to monoclinic $BiVO_4$ and FTO peaks, the diffraction data show broad background intensities between 15° and 40° of 2 theta values. This background is most pronounced at the smallest angle of incidence (0.1°) and can be observed more clearly when the intensity is plotted on a logarithmic scale (Fig. 2b) (see supporting information). This background indicates the presence of a quasi-amorphous phase in the films, which remains present even after the final heat-treatment at 460°C for two hours. However, this background decreases in intensity with increasing T_{PR}, indicating that heating to sufficiently high temperatures after deposition of each individual layer is essential for obtaining a fully crystalline multi-layer film. In other words, once a non- or partially-crystallized layer is covered by other layers, it can no longer be fully crystallized during the final heat treatment at 460°C. To further investigate this, we also did X-ray diffraction on multilayer films before doing the final heat treatment at 460°C (Fig. 3).

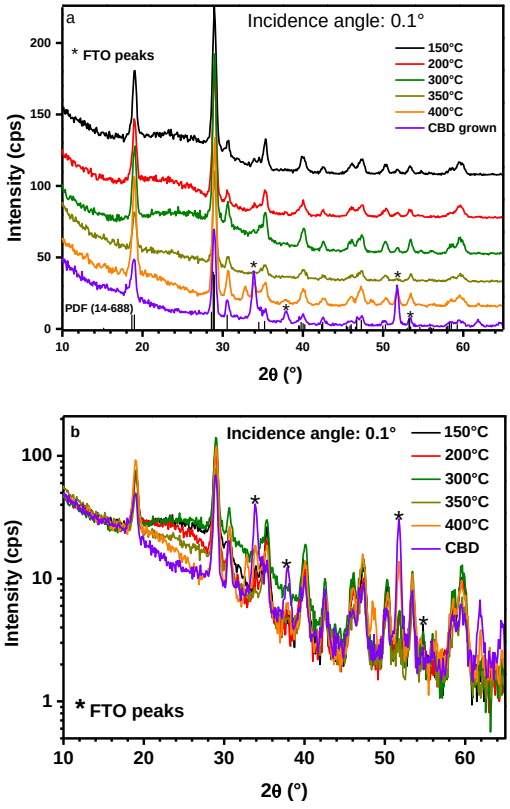

Figure 2. (a) XRD data for $BiVO_4$ electrodes made with different pre-heating temperatures, after a final heat treatment of 460°C. (b) The bottom graph shows the same data on a logarithmic scale in order to better illustrate the broad feature

between 20-40°. The XRD spectrum of chemical bath deposition (CBD)-grown $BiVO_4$ (highly crystalline) is also shown as a comparison.

The films pre-heated at 300°C are amorphous, whereas the films pre-heated at 350°C are already crystalline even before the final treatment at 460°C. After this final treatment no new peaks are observed (red curve), but the existing ones increase in intensity and become sharper, indicating a further increase in crystallinity and crystallite size, respectively, through coalescence during the partial sintering of the films as shown in figure 4 (b and d). To quantify this, we have integrated the total area of the XRD peaks; after the final heat treatment at 460°C (red curve), the integrated area under the peaks is 40% higher than the area before the treatment (blue curve). We also observe a 25% increase in the (full) peak width at half height (FWHM), but since these measurements are done in the grazing incidence configuration, we cannot extract reliable values for the crystallize size.

Morphological changes induced by increasing the pre-heating temperature T_{PR} are shown by the three representatives SEM micrographs in Fig. 4a-c. At a T_{PR} of 150°C, the $BiVO_4$ photoanodes show a diffuse morphology of a sponge-like network without sharp grain boundaries. The film keeps its sponge-like porous structure at T_{PR} value of 400 °C. However, the structure has coalesced into individual particles with a size between 30 and 120 nm, and the grain boundaries can be clearly observed. At an intermediate T_{PR} value of 350 °C, some degree of coalescence has occurred, but the individual grain boundaries cannot yet be observed. The film shows more porosity and a morphology that is intermediate between those of the films treated at 150 and 400°C. A T_{PR} of 350°C seems to be high enough to remove most organic components and leads to highly porous and crystalline $BiVO_4$ layers as shown in figure 4d. These layers coalesce during the final heat-treatment leading to less porous sponge-like network without clear grain boundaries (Fig. 4b).

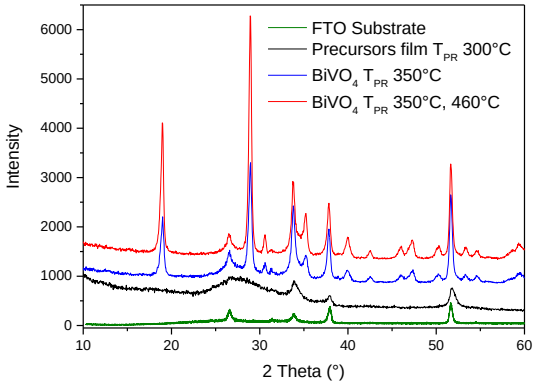

Fig. 3 XRD data of the multi-layer films pre-heated at different temperatures, but without the final heat treatment.

The effect of T_{PR} on the optical absorption was investigated using fused silica (quartz glass) as a substrate. The spin-coated films are bright yellow, optically transparent and show almost no scattering, indicating a highly homogeneous morphology (Fig 5). Figure 6 shows the evolution of the optical absorption as a function of the intermediate heating temperature T_{PR}. To isolate the effect of T_{PR} while still matching the processing conditions of the multi-layers, all spectra were recorded for a single spin-coated layer after heating for 10 min. at the indicated T_{PR}. Moreover, all layers were made from freshly prepared solutions. Fig. 6 clearly shows that a major change in the optical spectrum occurs between 340–350°C. At 340°C and below, the onset of absorption is at ~420 nm (2.9 eV). We attribute this high-energy absorption onset to the fact that the film is not yet fully crystallized (Fig. 3). At 350°C, a new absorption feature appears that shifts the onset of absorption to ~480 nm (2.6 eV), which corresponds to the well-established indirect bandgap of crystalline $BiVO_4$[29]. This indicates the critical importance of pre-heating solution-derived films to at least 350°C to achieve the nucleation and growth of the desired monoclinic scheelite phase of $BiVO_4$.

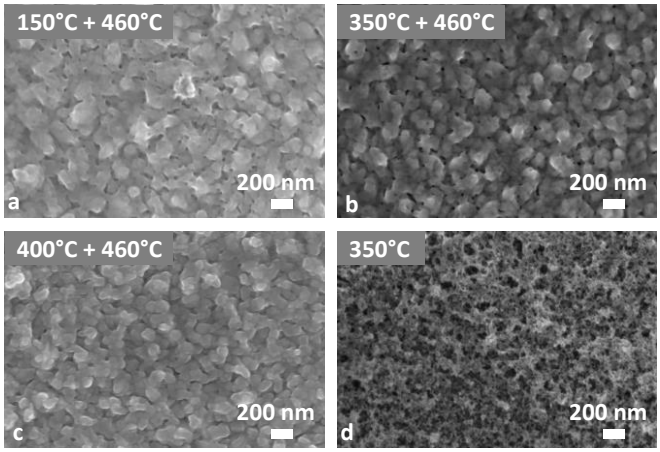

Figure 4. SEM images of $BiVO_4$ electrodes, consisting of 8 layers, processed at T_{pr} of 150°C, 350°C, and 400°C. All three electrodes underwent the same final heat-treatment at 460 °C. SEM image processed at T_{pr} of 350°C without further heating (bottom right).

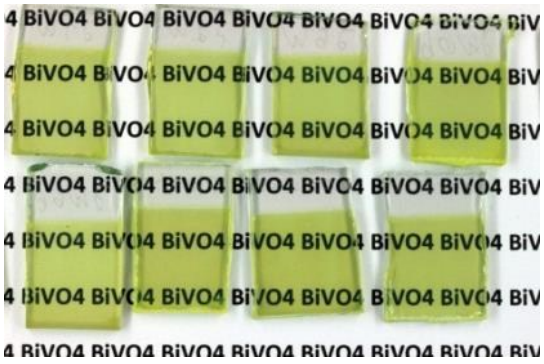

Fig. 5 Photograph showing the optical transparency of multilayer $BiVO_4$ electrodes (8 layers) prepared under the same conditions by spin-coating and after a final heat-treatment in air at 460°C.

Generally, the formation mechanism in such solid-state reactions is not well understood. The first critical step is pyrolysis of the organic components of organometallic bismuth

and vanadium precursors. At low temperatures (< 350°C) and short heating times (10 min.) the films presumably contain both inorganic as well as organic components in a (quasi) amorphous structure (black curve in Fig. 3). At higher temperatures and/or longer heating times, the organic components burn off, this allows the second step to take place; nucleation and growth of crystalline BiVO4. Whether or not these steps can also occur concurrently (i.e., in the same temperature window) and to what extent the kinetics of both steps differ is not well understood

The SEM observations of the preheated films at 300 ° indicate a segregation reaction and the formation of two types of objects (see Fig. S4, supporting information). During the preheating at lower temperatures such as in the case of 300°C, a masse transfer in the presence of organics takes place leading to the formation of two phases and to the loss of the homogeneous mixing at the molecular level obtained by spin-coating a homogeneous solution. This is probably due to a difference in the thermal behavior of the bismuth and vanadium in the presence of acetate and alkoxide ligands. After this segregation, the final heating at 460 °C, does not lead to a complete reaction between the two phases, explaining the formation of an amorphous content. However, introducing the spin-coated films in a preheated furnace at 350 °c leads to a fast pyrolysis of the organic avoiding such segregation and favor the reaction of bismuth and vanadium precursors homogeneously mixed at the molecular level.

3.2 Effect of pre-heating temperature on the photoelectrochemical properties of $BiVO_4$ photoanodes

The effect of the preheating temperature T_{PR} on the photoelectrochemical properties of $BiVO_4$ in the absence of an efficient hole scavenger, such as hydrogen peroxide, is shown in Fig. 7. In this case, the highest anodic photocurrents are obtained for a T_{PR} value of 350°C under both front- and back-side illumination. The next-highest photocurrents are found for a T_{PR} of 150°C. All other temperatures give much lower photocurrents, without any clear trend. Front-side illumination curves (Fig. S2 of the Supporting Information) look similar, but give slightly higher photocurrents. This is consistent with previous reports on undoped $BiVO_4$, which is known to give lower front-side photocurrents due to poor electronic conductivity[22]. In order to de-convolute different contributions to the photocurrent, photoelectrochemical measurements are performed in the presence of H_2O_2 as an efficient hole scavenger (Fig. 8, front-side illumination curves are shown in Fig. S3). Here, a different behaviour is observed. With H_2O_2, the catalytic limitation is removed, i.e. we are comparing the bulk carrier properties of our $BiVO_4$[13,20]. Figure 8 shows that photoelectrode processed at T_{PR} of 350 °C still shows the highest photocurrent; consistent with the results in the absence of H_2O_2. This indicates that this $BiVO_4$ photoelectrode exhibits better bulk properties as well as catalytic properties than the others. The $BiVO_4$ film processed at a T_{PR} of 400°C shows the second highest photocurrent in the presence of H_2O_2, despite showing the smallest photocurrent when H_2O_2 is not present. This indicates that the pre-heating at 400°C leads to $BiVO_4$ with good bulk charge separation properties, but the surface shows poor charge injection efficiency due to slow water oxidation kinetics.

It is important to note that the photocurrent values obtained are relatively low compared to those reported for Mo- or W-doped $BiVO_4$[8,11-13]. This is due to the poor conductivity of non-doped $BiVO_4$[13-15]. Moreover, no interfacial layer between the $BiVO_4$ and the back-contact (e.g. SnO_2[21,22], WO_3[23,24]), nor any co-catalyst (e.g. Co-Pi[25], FeOOH[26], NiOOH[16,26]) was used in these films. The lack of a water oxidation co-catalyst is also the cause of relatively positive onset potential in Fig. 7. These modifications are likely to further improve the activity of our films, but are beyond the scope of the current study.

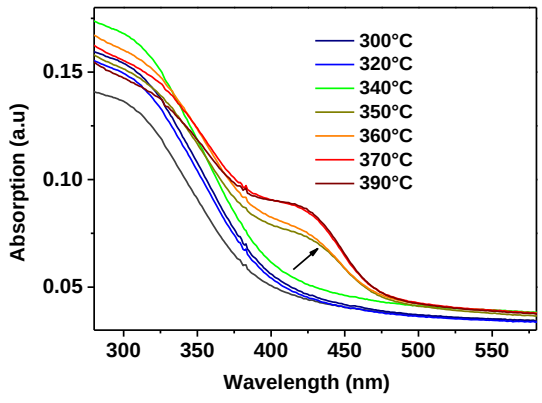

Fig. 6 Changes of UV-vis absorption spectra of precursors films on quartz substrates heated at different T_{pr}. The absorption feature that develops at T > 350°C corresponds to the expected band gap of crystalline $BiVO_4$.

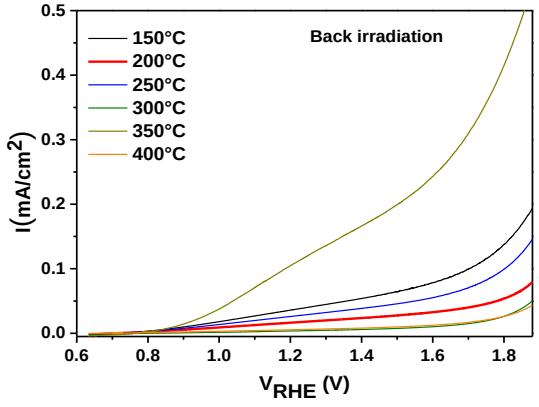

Fig. 7 Photocurrent-voltage measurement of $BiVO_4$ (8 layers) processed at different T_{pr} values under AM1.5 back-side illumination. The scan rate is 10 mV/s and the electrolyte is a 0.5 M K_2SO_4 solution buffered to pH 5.9.

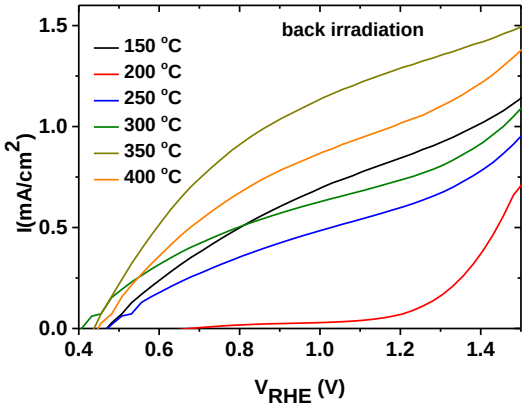

Fig. 8 Photocurrent-voltage measurement of non-doped $BiVO_4$ (8 layers) processed at different Tpr values under AM1.5 front-side illumination and in the presence of H_2O_2. The scan rate is 10 mV/s.

Figure 9 shows the photoelectrochemical behaviour of $BiVO_4$ photoanodes with different thicknesses (i.e., number of layers), made using the previously determined optimal preheating temperature of 350°C. From SEM cross-sections, a single layer corresponds roughly to a thickness of 10 nm. The electrodes are examined with linear sweep voltammograms under chopped back-side illumination, and H_2O_2 was used as a hole scavenger. Since the catalytic limitation is removed, the comparison of these photocurrents will only reflect the bulk properties. The 80 and 160 nm films show about the same anodic current for a bias between 1.25 and 1.4 V vs. RHE. For non-doped $BiVO_4$ in this thickness regime, the optical absorption increases with thickness, but charge transport efficiency decreases. For the 80 and 160 nm, these effects cancel each other, resulting in similar photocurrents. Further increase in thickness to 240 nm leads to a clear decrease in anodic photocurrent due to charge transport limitations in this non-doped $BiVO_4$.

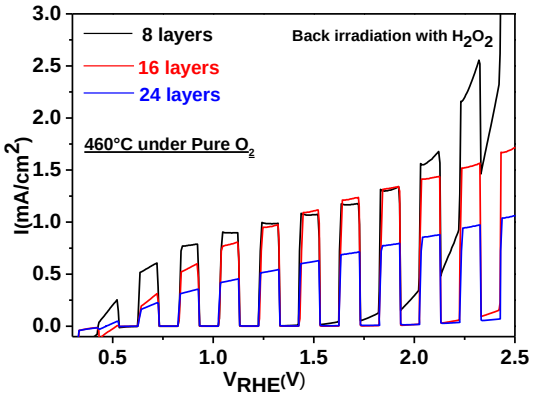

Fig. 9 Photocurrent-voltage measurement of non-doped $BiVO_4$ electrodes with different thicknesses (80, 160 and 240 nm).

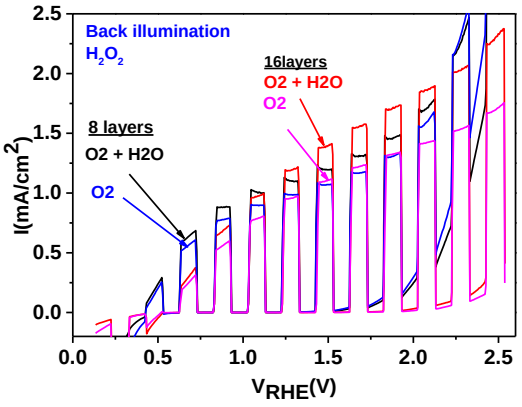

Fig. 10 Photocurrent-voltage measurement of non-doped $BiVO_4$ electrodes with a final heating under pure oxygen and oxygen with water vapor.

A small increase in anodic photocurrent is observed if the final calcination is performed under a mixture of oxygen and water vapor instead of pure oxygen. Hébrard et al reported an accelerating effect of water vapour and oxygen on the sintering and grain-boundary diffusion for titania[27]. A similar effect may occur in our BiVO4 electrodes, and lead to improved connectivity between the grains. This would lead to better charge transport. As shown in Fig. 10, the effect becomes more pronounced for thicker films. This is indeed consistent with the explanation above, since grain boundary resistances will become more important as the film thickness increases.

Conclusion

The results presented in this paper demonstrate the importance of intermediate heat treatments during the solution processing of multi-layered (undoped) thin film $BiVO_4$ photoanodes. We find that for 10 min. heat treatments below 350°C the layers remain X-ray amorphous and show a significant blue-shift of the optical absorption onset compared to that of crystalline $BiVO_4$. The multilayer film can be converted into crystalline $BiVO_4$ by a final anneal at 460°C, but a significant amount of quasi-amorphous material remains. In contrast, intermediate heat treatments at $T_{PR} \geq 350$°C for 10 min. result in complete crystallization of the films into the desired monoclinic scheelite phase. The highest photocurrents are observed for a T_{PR} of 350°C; pre-heating at a higher temperature (400°C) improves the charge transport properties of the film, but reduces the injection efficiency into the electrolyte. We also find that the connectivity between the grains can be improved by performing the final anneal in a mixture of oxygen and water vapor, resulting in slightly higher photocurrents. These findings offer a first glimpse at how intermediate drying and heating conditions affect the performance of solution-processed $BiVO_4$ photoelectrodes. A more detailed understanding of the rearrangements at the atomic scale would be the next step toward the development of efficient metal oxide-based light absorbers with low-cost solution-based processes.

Acknowledgements
We thank Ulricke Bloeck for taking some SEM pictures.

Notes and references

Institute for Solar Fuels , Helmholtz-Zentrum Berlin für Materialien und Energie GmbH, Hahn-Meitner-Platz 1, 14109 Berlin (Germany)
*E-Mail:Chemseddine@helmholtz-berlin.de

1 F. E. Osterloh, B.A. Parkinson, MRS Bulletin, 2011, 36, 17.
2 A. Fujishima, K. Honda, Nature, 1972, **238**, 37.
3 O. Khaselev, J. A. Turner, Science, 1998, 280, 425.
4 J. Brillet, J.-H. Yum, M. Cornuz, T. Hisatomi, R. Solarska, J. Augustynski, M. Graetzel, K. Sivula, Nat. Photon. 2012, 6, 824.
5 F. F. Abdi, L. Han, A. H. M. Smets, M. Zeman, B. Dam, R. van de Krol, Nat. Commun. 2013, 4:2195.
6 Y. Park, K.J. McDonald, K. Choi, Chem. Soc. Rev. 2013, 42, 2321.
7 L. Chen, E. Alarcón-Liadó, M. Hettick, I.D. Sharp, Y. Lin, A. Javey, J.W. Ager. J. Phys. Chem. C 2013, 117, 21635.
8 L. Chen, F. M. Toma, J. K. Cooper, A. Lyon, Y. Lin, I. D. Sharp, J. W. Ager, ChemSusChem 2015, 8, 1066.
9 Y. Liang, T. Tsubota. L.P.A. Mooij, R. van de Krol. . J. Phys. Chem. C 2011, 115, 17594.
10 F. F. Abdi, N. Firet, A. Dabirian, R. van de Krol, MRS Proceedings, 2012, 1446 mrss12-1446-u02-05 doi:10.1557/opl.2012.811.
11 D.K. Zhong, S. Choi, D.R. Gamelin, J. Am. Chem. Soc. 2011, 133, 18370.
12 W. Luo, Z. Yang, Z. Li, J. Zhang, J. Liu, Z. Zhao, Z. Wang, S. Yan, T. Yu, Z. Zou, Energy Environ. Sci., 2011, 4, 4046.
13 F.F. Abdi, N. Firet, R. van de Krol. ChemCatChem 2013, 5, 490.
14 J.A. Seabold, K. Zhu, N.R. Neale. Phys. Chem. Chem. Phys. 2014, 16. 1121.
15 S.P. Berglund, A.J.E. Rettie, S. Hoang, C.B. Mullins. Phys. Chem. Chem. Phys. 2012, 14, 7065.
16 T.W. Kim, K.S. Choi, Science 2014, 343, 990.
17 X. Shi, I.Y. Choi, K. Zhang, J. Kwon, D.Y. Kim, J. K. Lee, S.H. Oh, J.K. Kim, J.H. Park, Nature Comm. 2014, Sep 2;5:4775. doi: 10.1038/ncomms5775.
18 Li. Zhang, E. Reisner, J. J. Baumberg Energy Environ. Sci., 2014, 7, 1402
19 L. Zhang, C.Y. Lin, V. K. Valev , E. Reisner , U. Steiner, J. J. Baumberg. Small, 2014, 10, 19, 3970
20 H. Dotan, K. Sivula, M. Gratzel, A. Rothschild and S. C. Warren, Energy Environ. Sci., 2011, 4, 958–964.
21 P. Chatchai, Y. Murakami, S.-y, Kishioka, A.Y. Nosaka, Y. Nosaka, Electrochem. Solid-State Lett 2008, 11, H160-H163.
22 Y. Liang, T. Tsubota, L.P.A. Mooij, R. van de Krol, J. Phys. Chem. C 2011, 115, 17594-17598.
23 R. Saito, Y. Miseki, K. Sayama, Chem. Commun. 2012, 48, 3833-3835.
24 P. Chatchai, S.-y. Kishioka, Y. Murakami, A. Y. Nosaka, Y. Nosaka, Electrochem. Acta, 2010, 55, 592-596.
25 F.F.Abdi, R. van de Krol, J. Phys. Chem. C 2012, 116, 9398-9404.
26 J. A. Seabold, K. Choi, J. Am. Chem. Soc. 2012, 134, 2186-2192
27 J.-L. Hébrard, P. Nortier, M. Pijolat, M. Soustelle, J. Am. Ceram. Soc. 1990, 73, 79-84.
28 M.C. Neves, T. Trindade, Thin Solid Films 2002, 406, 93.
29 J.K. Cooper, S. Gul, F.M. Toma, L. Chen, Y.S. Liu, J. Guo, J.W. Ager, J. Yano, I.D. Sharp. J. Phys. Chem. C 2015, 119, 2969